Hydrothermal Syntheses and Structural Characterization of Layered Vanadium Oxides Incorporating Organic Cations: α-, β-$(H_3N(CH_2)_2NH_3)[V_4O_{10}]$ and α-, β-$(H_2N(C_2H_4)_2NH_2)[V_4O_{10}]$

Yiping Zhang,[†,‡] Robert C. Haushalter,*[,‡] and Abraham Clearfield*[,†]

NEC Research Institute, 4 Independence Way, Princeton, New Jersey 08540, and Department of Chemistry, Texas A&M University, College Station, Texas 77843

Received September 26, 1995[⊗]

Four new layered mixed-valence vanadium oxides, which contain interlamellar organic cations, α-$(H_3N(CH_2)_2NH_3)[V_4O_{10}]$ (**1a**), β-$(H_3N(CH_2)_2NH_3)[V_4O_{10}]$ (**1b**), α-$(H_2N(C_2H_4)_2NH_2)[V_4O_{10}]$ (**2a**), and β-$(H_2N(C_2H_4)_2NH_2)[V_4O_{10}]$ (**2b**), have been prepared under hydrothermal conditions and their single-crystal structures determined: **1a**, triclinic, space group $P\bar{1}$, $a = 6.602(2)$ Å, $b = 7.638(2)$ Å, $c = 5.984(2)$ Å, $\alpha = 109.55(3)°$, $\beta = 104.749(2)°$, $\gamma = 82.31(3)°$, $Z = 1$; **1b**, triclinic, $P\bar{1}$, $a = 6.387(1)$ Å, $b = 7.456(2)$ Å, $c = 6.244(2)$ Å, $\alpha = 99.89(2)°$, $\beta = 102.91(2)°$, $\gamma = 78.74(2)°$, $Z = 1$; **2a**, triclinic, $P\bar{1}$, $a = 6.3958(5)$ Å, $b = 8.182(1)$ Å, $c = 6.3715(7)$ Å, $\alpha = 105.913(9)°$, $\beta = 104.030(8)°$, $\gamma = 94.495(8)°$, $Z = 1$; **2b**, monoclinic, space group $P2_1/n$, $a = 9.360(2)$ Å, $b = 6.425(3)$ Å, $c = 10.391(2)$ Å, $\beta = 105.83(1)°$, $Z = 2$. All four of the compounds contain mixed-valence V^{5+}/V^{4+} vanadium oxide layers constructed from $V^{5+}O_4$ tetrahedra and pairs of edge-sharing $V^{4+}O_5$ square pyramids with protonated organic amines occupying the interlayer space.

Introduction

The contemporary interest in vanadium oxide bronzes reflects not only their interesting electronic and magnetic properties[1] but also their complex structural chemistry, associated with the ability of vanadium to adopt a variety of coordination geometries in various oxidation states. In addition to the conventional alkali-metal bronzes $A_xV_2O_5$,[2] a class of organic-based vanadium bronzes are also known. While most of the alkali-metal bronzes have been prepared at high temperatures, the organic-based vanadium bronzes are prepared at room temperature or slightly higher via intercalation reactions with vanadium pentoxide xerogels, $V_2O_5 \cdot nH_2O$. The $V_2O_5 \cdot nH_2O$ host possesses a porous layered structure and is capable of intercalating a variety of neutral and charged guest species such as alkali-metal ions,[3] alkylamines,[4] alcohols,[5] pyridine,[6] benzidine,[7] etc. The insertion of amines or metal complexes into V_2O_5 hosts has also been reported.[8] The resulting intercalation compounds usually retain the lamellar structure with the guest species and water molecules occupying the interlayer regions. Partial reduction of V^{5+} to V^{4+} of the oxide layers has been observed to accompany the intercalation reactions with organic amines. In the cases of aniline[9] and thiophene,[10] the reduction of the vanadium oxide host, and the simultaneous oxidative polymerization of the guest molecules in the interlayer regions, have been observed. These intercalation compounds with reduced vanadium sites constitute an interesting class of organic−inorganic composite materials that can be viewed as molecular or polymer vanadium bronzes by analogy to alkali-metal bronzes.[2] However, the structural information about these intercalation compounds is very limited due to their amorphous or semicrystalline nature and lack of high-quality single crystals.

Hydrothermal techniques, in combination with organic templates, have been recently demonstrated to be well suited for the synthesis and crystal growth of reduced oxomolybdenum and oxovanadium phosphates and vanadium phosphonates. A series of novel organically templated molybdenum and vanadium phosphates and vanadium phosphonates with molecular, two-dimensional layered, and three-dimensional open-framework structures have been prepared under hydrothermal conditions.[11] In contrast, hydrothermal synthesis of vanadium oxides using organic templates remains relatively unexplored.[12] While there are many examples of alkali-metal vanadium oxide bronzes with three-dimensional or two-dimensional structures in which the alkali metals occupy the channels or the interlayer regions, analogous organically templated vanadium oxides with 3-D open

* To whom all correspondence should be addressed.
† Texas A&M University.
‡ NEC Research Institute.
⊗ Abstract published in *Advance ACS Abstracts,* August 1, 1996.

(1) Murphy, D. W.; Christian, P. A. *Science* **1979**, *205*, 651.
(2) Hagenmuller, P. In *Non-Stoichiometric Compounds, Tungsten Bronzes, Vanadium Bronzes and Related compounds*; Bevan, D. J., Hagenmuller, P., Eds.; Pergamon Press: Oxford, U.K., 1973; Vol. 1.
(3) Lemordant, D.; Bouhaouss, A.; Aldebert, P.; Baffier, N. *Mater. Res. Bull.* **1986**, *21*, 273.
(4) Paul-Boucour, V.; Aldebert, P. *Mater. Res. Bull.* **1983**, *18*, 1247.
(5) Aldebert, P.; Baffier, N.; Legendre, J.-J.; Livage, J. *Rev. Chim. Miner.* **1982**, *19*, 485. Aldebert, P.; Baffier, N.; Gharbi, N.; Livage, J. *Mater. Res. Bull.* **1981**, *16*, 949. Lemordant, D.; Bouhaouss, A.; Aldebert, P.; Baffier, N. *J. Chim. Phys. Phys.-Chim. Biol.* **1986**, *83*, 105.
(6) Ruiz-Hitzky, E.; Casal, B. *J. Chem. Soc., Faraday Trans. 1* **1986**, *82*, 1597.
(7) Hasbah, H.; Tinet, D.; Crespin, M. M.; Erre, R.; Setton, R.; Van Damme, H. *J. Chem. Soc., Chem. Commun.* **1985**, 935.
(8) Kanatzidis, M.; Marks, T. J. *Inorg. Chem.* **1987**, *26*, 783 and references therein.
(9) Kanatzidis, M.; Wu, C.-G. *J. Am. Chem. Soc.* **1989**, *111*, 4139.
(10) Kanatzidis, M.; Wu, C.-G.; Marcy, H. O.; DeGroot, D. C.; Kannewurf, C. R. *Chem. Mater.* **1990**, *2*, 222.
(11) Haushalter, R. C.; Mundi, L. A. *Chem. Mater.* **1992**, *4*, 31. Soghomonian, V.; Chen, Q.; Haushalter, R. C.; Zubieta, J.; O'Connor, C. J. *Science* **1993**, *259*, 1596. Soghomonian, V.; Chen, Q.; Haushalter, R. C.; Zubieta, J. *Angew. Chem., Int. Ed. Engl.* **1993**, *32*, 610. Soghomonian, V.; Chen, Q.; Haushalter, R. C.; Zubieta, J. *Chem. Mater.* **1993**, *5*, 1690. Soghomonian, V.; Chen, Q.; Haushalter, R. C.; Zubieta, J., *Chem. Mater.* **1993**, *5*, 1595. Soghomonian, V.; Haushalter, R. C.; Chen, Q.; Zubieta, J. *Inorg. Chem.* **1994**, *33*, 1700. Zhang, Y.; Clearfield, A.; Haushalter, R. C. *J. Solid State Chem.* **1995**, *117*, 157. Zhang, Y.; Clearfield, A.; Haushalter, R. C. *Chem. Mater.* **1995**, *7*, 1221.
(12) Huan, G.-H.; Johnson, J. W.; Jacobson, A. J.; Merola, J. S. *J. Solid State Chem.* **1991**, *91*, 385. Duan, C.-Y.; Tian, Y.-P.; Lu, Z.-L.; You, X.-Z.; Huang, X.-Y. *Inorg. Chem.* **1995**, *34*, 1.

S0020-1669(95)01237-7 CCC: $12.00

frameworks have not been observed so far. Inspired by our successful investigation into the hydrothermal synthesis of new reduced vanadium phosphates, we sought to explore the hydrothermal synthesis of new reduced vanadium oxides using organic templates. Along these lines, two novel layered vanadium oxides, $(H_3N(CH_2)_3NH_3)[V_4O_{10}]$[13] and $(HN(C_2H_4)_3NH)[V_6O_{14}]\cdot H_2O$,[14] have been isolated and structurally characterized by X-ray crystallography. While both compounds contain a layered structure with the organic cations occupying the interlayer regions, the oxide layers in the two structures differ substantially in their composition, connectivity, degree of reduction, and thus electronic and magnetic properties, which reflects the difference in the nature of the two organic cations. In addition, we have discovered a large class of layered vanadium oxide materials with metal coordination complexes (e.g. M(L)$_2$: (M = Ni, Cu, Zn; L = ethylenediamine, 1,3-diaminopropane) between the VO layers.[15] In an effort to further investigate the influence of organic templates on the structures of layered vanadium oxides, we have obtained α-$(H_3NCH_2CH_2NH_3)[V_4O_{10}]$ (**1a**), β-$(H_3NCH_2CH_2NH_3)[V_4O_{10}]$ (**1b**), α-$(H_2N(C_2H_4)_2NH_2)[V_4O_{10}]$ (**2a**), and β-$(H_2N(C_2H_4)_2NH_2)[V_4O_{10}]$ (**2b**). The syntheses and single-crystal structures of these compounds are reported here. All of these compounds contain mixed-valence V^{5+}/V^{4+} oxide layers with organic cations occupying the interlayer space.

Experimental Section

Materials and Methods. Chemicals used were of reagent grade quality and were obtained from commercial sources and used without further purification. The powder X-ray diffraction patterns were obtained on a Scintag XDS 2000 diffractometer with Cu Kα radiation (λ = 1.5418 Å). Thermogravimetric analyses (TGA) were carried out with a Perkin-Elmer TGA 7 thermal analysis system at a heating rate of 10 °C/min under an N_2 atmosphere. The EDS analyses were performed on a Hitachi S-2700 SEM. The hydrothermal reactions were carried out in Parr acid digestion bombs with 23 mL poly(tetrafluoroethylene) liners.

Synthesis of α- and β-$(H_3NCH_2CH_2NH_3)[V_4O_{10}]$. A mixture of V_2O_5 (0.173 g), ethylenediamine (0.10 mL), and H_2O (10 mL) with a mole ratio of 1.0:1.57:585 was sealed in a digestion bomb which was heated at 170°C for 121 h. Black rod-shaped crystals (0.1 g) were isolated after filtering, washing with water, and air-drying. Powder X-ray diffraction studies indicated that these crystals are a mixture of **1a** and **1b**, even though they were quite similar in appearance. After examination of several crystals for single-crystal X-ray diffraction studies, the crystals were found to have two sets of distinctive unit cells which corresponded to **1a** and **1b**. The optimum conditions for preparation of a single phase of α- or β-form have not been found.

Synthesis of α- and β- $(H_2N(C_2H_4)_2NH_2)[V_4O_{10}]$. A hydrothermal reaction of 0.216 g of $NaVO_3$, 0.346 g of $H_2O_3PCH_3$, 0.232 g of piperazine, and 10 mL of H_2O in a mole ratio of 1.0:3.0:2.3:266 at 170 °C for 47 h yielded 0.14 g of thin black plates after filtering, washing with water, and air-drying. The presence of $H_2O_3PCH_3$ in the starting materials serves to increase the acidity of the solution. The pH of the solution before the reaction and at completion was around 7. Other acids such as HCl also serve in this capacity. The EDS analysis of these crystals showed the presence of only V. Powder X-ray diffraction studies indicated that these thin plates are a mixture of **2a** and **2b**. This was further confirmed by single-crystal X-ray diffraction studies on several single crystals selected, which were found to have two distinctive unit cells corresponding to **2a** and **2b**.

X-ray Crystallographic Study. In each of the four studies, a suitable crystal was mounted on a glass fiber. All measurements were made at room temperature on a Rigaku AFC7R diffractometer with graphite-monochromated Mo Kα radiation and an 18 kW rotating anode generator. Cell constants and an orientation matrix for data collection were obtained from a least-squares refinement using the setting angles of 24−25 carefully centered reflections in the range $20° < 2\theta < 30°$. Data were collected in the range $5° < 2\theta < 60°$ using the $\omega-2\theta$ scan technique. In all cases only a unique portion of the reflections were collected. The intensities of three representative reflections which were measured after every 150 reflections remained constant throughout data collection. Empirical absorption corrections based on ψ-scan measurements were applied. In the case of **2b**, an empirical absorption correction using the program DIFABS[16] was applied. The data were corrected for Lorentz and polarization effects, and the structures were solved by direct methods. The non-hydrogen atoms were refined anisotropically. All the hydrogen atoms were located from difference Fourier maps and included in the refinement with fixed positional and thermal parameters. Neutral atom scattering factors were taken from Cromer and Waber.[17] Anomalous dispersion effects were included, and the values for $\Delta f'$ and $\Delta f''$ were those of Cromer.[18] All structures were refined on the basis of independent reflections with $I \geq 3\sigma(I)$ by full-matrix least squares using the teXsan program package.[19] Experimental crystallographic data for **1a**, **1b**, **2a**, and **2b** are listed in Table 1.

Table 1. Crystallographic Data for Oxides **1a**, **1b**, **2a**, and **2b**

	1a	**1b**	**2a**	**2b**
empirical formula	$V_2O_5NCH_5$	$V_2O_5NCH_5$	$V_2O_5NC_2H_6$	$V_2O_5NC_2H_6$
fw	212.94	212.94	225.96	225.96
a (Å)	6.602(2)	6.387(1)	6.3958(5)	9.360(2)
b (Å)	7.638(2)	7.456(2)	8.182(1)	6.425(3)
c (Å)	5.984(2)	6.244(2)	6.3715(7)	10.391(2)
α (deg)	109.55(3)	99.89(2)	105.913(9)	90
β (deg)	104.749(2)	102.91(2)	104.030(8)	105.83(1)
γ (deg)	82.31(3)	78.74(2)	94.495(8)	90
V (Å^3)	274.6(2)	281.7(1)	307.29(7)	601.2(3)
Z	2	2	2	4
space group	$P\bar{1}$(No. 2)	$P\bar{1}$(No. 2)	$P\bar{1}$(No. 2)	$P2_1/n$ (No. 14)
D_c (g/cm^3)	2.575	2.510	2.442	2.496
T (°C)	20 ± 1	20 ± 1	20 ± 1	20 ± 1
λ(Mo Kα) (Å)	0.7107	0.7107	0.7107	0.7107
μ (cm^{-1})	33.46	32.62	29.98	30.65
R[a]	0.030	0.022	0.033	0.033
R_w[a]	0.035	0.026	0.040	0.036

[a] $R = \sum||F_o| - |F_c||/\sum|F_o|$ and $R_w = (\sum w(|F_o| - |F_c|)^2/\sum wF_o^2)^{1/2}$.

Results

Positional and thermal parameters of the atoms in the structures of **1a** are given in Table 2, and selected bond distances and angles in Table 3. Figure 1 shows the layered nature of the structure of **1a**, consisting of vanadium oxide layers with ethylenediammonium dications occupying the interlamellar space between the layers, and a view perpendicular to one of the vanadium oxide layers. Each oxide layer is constructed from equal numbers of VO_4 tetrahedra and VO_5 square pyramids. While the VO_4 tetrahedra are isolated from each other, the VO_5 square pyramids exist in pairs sharing a common edge. Within a pair of square pyramids, the two apical oxygen atoms are oriented toward opposite sides of the plane of the layer. Each pair of the pyramids is linked to six VO_4 tetrahedra via corner sharing, forming a two-dimensional layer with a composition of $V_4O_{10}^{2-}$. Figure 2 shows the coordination environment of the V atoms in the asymmetric unit and the numbering scheme used in Table 3. The V(1)O_5 group is a distorted square pyramid

(13) Zhang, Y.; O'Connor, C. J.; Clearfield, A.; Haushalter, R. C. *Chem. Mater*. **1996**, *8*, 595.
(14) Zhang, Y.; Clearfield, A.; Haushalter, R. C. *J. Chem. Soc., Chem. Commun.* **1996**, 1055.
(15) Zhang, Y.; DeBord, J. R. D.; O'Connor, C. J.; Haushalter, R. C.; Zubieta, J.; Clearfield, A. *Angew. Chem., Int. Ed. Engl.* **1996**, *35*, 989.
(16) Walker, N.; Stuart, D. *Acta Crystallogr.* **1983**, *A39*, 158.
(17) Cromer, D.; Waber, J. T. *International Tables for X-ray Crystallography*; Kynoch Press: Bimingham, U.K., 1974; Vol. IV, Table 2.2A.
(18) Cromer, D. T. Reference 16, Table 2.3.1.
(19) teXsan: Texray Structural Analysis Package; Molecular Structure Corp., The Woodlands, TX, 1992 (revised).

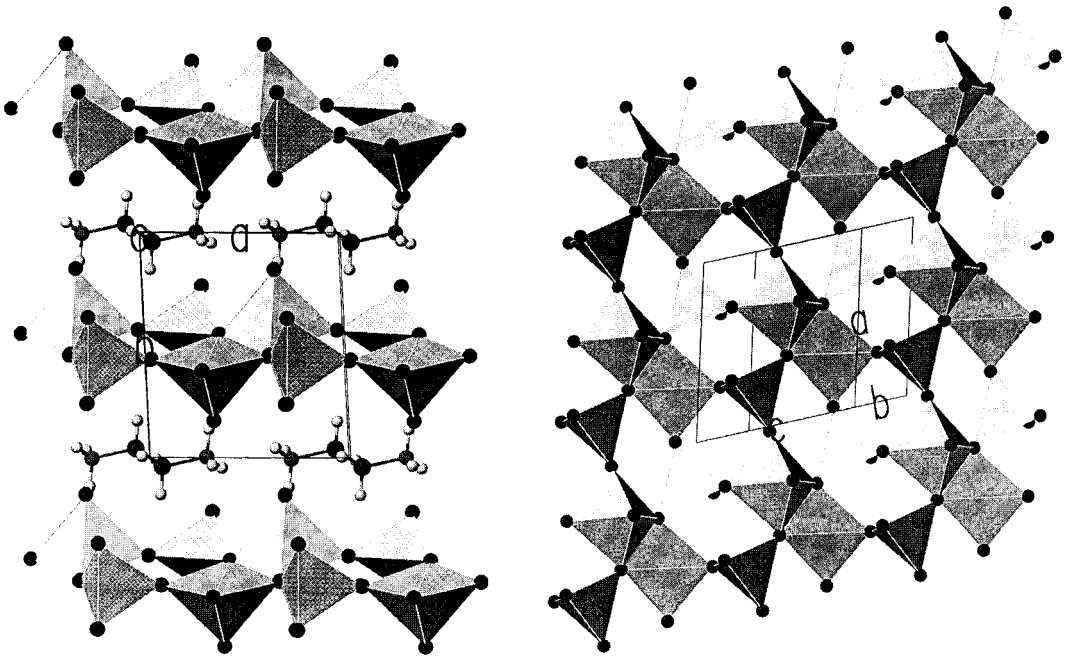

Figure 1. (left) View of the structure of **1a** down the *c* axis showing the layers of vanadium oxide and the ethylenediammonium dications in the interlamellar space. (right) View perpendicular to the oxide layer in the structure of **1a**.

Table 2. Positional Parameters and *B*(eq) Values (Å^2) for Oxides **1a**, **1b**, **2a**, and **2b**

atom	*x*	*y*	*z*	*B*(eq)[a]	atom	*x*	*y*	*z*	*B*(eq)[a]
				Compound **1a**					
V(1)	0.68007(8)	0.37874(8)	0.60083(10)	0.895(10)	O(4)	0.3778(3)	0.4529(3)	0.5962(4)	1.19(4)
V(2)	1.23102(9)	0.42999(8)	0.80443(10)	0.919(10)	O(5)	1.3031(4)	0.2373(4)	0.8694(5)	1.95(5)
O(1)	0.9712(4)	0.4335(4)	0.6784(4)	1.86(5)	N(1)	0.2887(5)	−0.0049(4)	0.1181(6)	2.02(6)
O(2)	0.7184(4)	0.3819(3)	0.9318(4)	1.33(4)	C(1)	0.0653(6)	0.0397(5)	0.1265(7)	1.89(7)
O(3)	0.6690(4)	0.1650(4)	0.4319(5)	1.92(5)					
				Compound **1b**					
V(1)	0.71619(6)	0.56232(5)	−0.15465(6)	0.790(7)	O(4)	0.6998(3)	0.7714(2)	−0.0226(3)	1.76(4)
V(2)	0.84493(6)	0.38780(5)	−0.66948(6)	0.795(7)	O(5)	0.8237(3)	0.3933(2)	0.0175(3)	1.08(3)
O(1)	0.8842(3)	0.1741(2)	−0.6354(3)	1.86(4)	N(1)	0.7110(4)	0.0611(3)	0.7491(4)	1.95(5)
O(2)	0.8677(3)	0.5387(2)	−0.3760(3)	1.15(3)	C(1)	0.5048(5)	0.0845(3)	0.5851(4)	1.79(5)
O(3)	0.4631(3)	0.5232(3)	−0.2821(3)	1.43(3)					
				Compound **2a**					
V(1)	0.8050(1)	0.39740(10)	0.8032(1)	0.79(1)	O(4)	0.7833(5)	0.4113(4)	0.5020(5)	1.29(6)
V(2)	0.2577(1)	0.43868(10)	0.6453(1)	0.83(1)	O(5)	0.7635(6)	0.1930(5)	0.7704(6)	1.95(8)
O(1)	0.5286(5)	0.4758(5)	0.7786(6)	1.69(7)	N(1)	0.4884(8)	0.0984(6)	0.2174(7)	1.89(9)
O(2)	1.1186(5)	0.4754(4)	0.8710(5)	1.09(6)	C(1)	0.6955(9)	0.0392(8)	0.1873(9)	2.1(1)
O(3)	0.1954(6)	0.2429(5)	0.4768(6)	1.96(7)	C(2)	0.6478(9)	−0.1229(7)	−0.008(1)	2.1(1)
				Compound **2b**					
V(1)	0.35340(6)	0.61669(8)	0.44859(5)	0.783(9)	O(4)	0.3667(3)	0.9131(4)	0.4599(2)	1.31(4)
V(2)	0.59045(6)	0.90167(8)	0.64969(5)	0.887(9)	O(5)	0.4852(3)	0.9930(4)	0.7373(3)	1.66(5)
O(1)	0.5437(3)	0.6342(4)	0.5856(2)	1.19(4)	N(1)	1.0211(5)	0.2034(6)	0.4557(5)	3.09(9)
O(2)	0.2592(3)	0.6431(4)	0.2607(3)	1.31(4)	C(1)	1.1112(5)	0.1303(7)	0.5865(5)	2.35(8)
O(3)	0.2250(3)	0.5502(4)	0.5185(3)	1.59(5)	C(2)	0.9658(6)	0.0384(8)	0.3600(4)	2.86(9)

[a] $B_{eq} = {}^8/_3\pi^2(U_{11}(aa^*)^2 + U_{22}(bb^*)^2 + U_{33}(cc^*)^2 + 2U_{12}aa^*bb^*\cos\gamma + 2U_{13}aa^*cc^*\cos\beta + 2U_{23}bb^*cc^*\cos\alpha)$.

with the shortest bond distance of 1.607(3) Å formed with the terminal oxygen O(3), while the base of the square pyramid has four V−O bond distances in the range of 1.924(2)−1.996(2) Å. The V(2)O_4 group has a tetrahedral configuration with V−O bond distances in the range of 1.626(3)−1.824(2) Å, and fairly regular bond angles in the range of 107.9(1)−110.1(1)°. While the square-pyramidal vanadium has an oxidation state of +4, the tetrahedral vanadium is indicative of an oxidation state of +5. This assignment of oxidation states is consistent with the overall charge balance of the compound and is confirmed by the valence sum calculation,[20] which gave a value of 4.1 for V(1) and 4.7 for V(2). There are three types of oxygen atoms in terms of bonding: O(3) and O(5) are terminal oxygens, O(1) and O(2) are two-coordinate, and O(4) is three-coordinate. An interesting feature of the structure of **1a** is that the ethylenediammonium dications in the interlayer space lie parallel with respect to the mean plane of vanadium oxide layers. The parallel packing of the amine molecules in the interlayer space is also reported for the superconducting host 2H-TaS_2 intercalated with $C_nH_{2n+1}NH_2$ ($n < 4$), although the structural details are not known.[21] The ethylenediammonium cations in **1a** form several strong hydrogen bonds with the adjacent vanadium oxide layers. The N atoms of the templates are hydrogen-bonded to the O atoms of the VO layers, as indicated by the contacts with oxygen atoms O(2) and O(3) from the upper

(20) Brown, I. D.; Altermatt, D. *Acta Crystallogr.* **1985**, *B41*, 244.

(21) Gamble, F. R.; Osiecki, J. M.; Cais, M.; Pisharody, R.; DiSalvo, F. J.; Geballe, T. H. *Science* **1971**, *174*, 493.

Table 3. Selected Bond Distances (Å) and Angles (deg) in the Structure of **1a**

V(1)−O(1)	1.928(3)	V(1)−O(2)	1.924(2)
V(1)−O(3)	1.607(3)	V(1)−O(4)	1.996(2)
V(1)−O(4A)	1.961(3)	V(2)−O(1)	1.689(2)
V(2)−O(2A)	1.735(2)	V(2)−O(4C)	1.824(2)
V(2)−O(5)	1.626(3)	N(1)−C(1)	1.479(5)
C(1)−C(1A)	1.505(7)		
O(1)−V(1)−O(2)	87.6(1)	O(1)−V(1)−O(3)	105.3(1)
O(1)−V(1)−O(4)	152.5(1)	O(1)−V(1)−O(4A)	87.7(1)
O(2)−V(1)−O(3)	107.4(1)	O(2)−V(1)−O(4)	88.5(1)
O(2)−V(1)−O(4A)	141.0(1)	O(3)−V(1)−O(4)	101.8(1)
O(3)−V(1)−O(4A)	111.2(1)	O(4)−V(1)−O(4A)	78.4(1)
O(1)−V(2)−O(2A)	109.0(1)	O(1)−V(2)−O(4C)	110.1(1)
O(1)−V(2)−O(5)	109.6(1)	O(2A)−V(2)−O(4C)	107.9(1)
O(2A)−V(2)−O(5)	109.7(1)	O(4C)−V(2)−O(5)	110.6(1)
N(1)−C(1)−C(1)	108.2(4)		

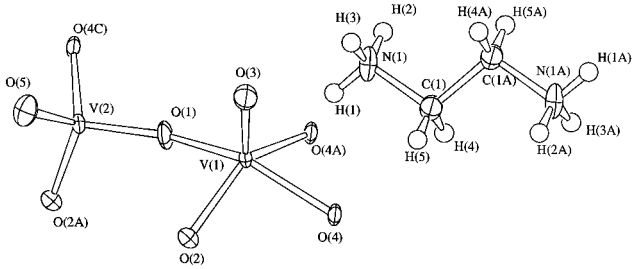

Figure 2. ORTEP drawing of the asymmetric unit in the structure of **1a** showing the coordination environment around the V atoms. The atoms labeled with A and C are symmetry-related atoms.

oxide layer and O(5) from the lower oxide layer, with N- - -O distances in the range of 2.759(4)−2.890(4) Å.

The positional and thermal parameters of the atoms in the structure of **1b** are given in Table 2, and selected bond distances and angles in Table 4. As shown in Figure 3, oxide **1b** has a layered structure similar to that found in **1a**. The oxide layer is constructed from VO_4 tetrahedra and VO_5 square pyramids in a similar manner. The coordination environment around the two independent V atoms in the asymmetric unit and the numbering scheme used in Table 4 is shown in Figure 4. The $V(1)O_4$ tetrahedron has bond distances in the range of 1.630

Table 4. Selected Bond Distances (Å) and Angles (deg) in the Structure of **1b**

V(1)−O(2)	1.824(2)	V(1)−O(3)	1.691(2)
V(1)−O(4)	1.630(2)	V(1)−O(5)	1.736(2)
V(2)−O(1)	1.607(2)	V(2)−O(2)	1.970(2)
V(2)−O(2A)	1.964(2)	V(2)−O(3A)	1.923(2)
V(2)−O(5A)	1.936(2)	N(1)−C(1)	1.478(4)
C(1)−C(1A)	1.504(5)		
O(2)−V(1)−O(3)	105.64(8)	O(2)−V(1)−O(4)	110.36(8)
O(2)−V(1)−O(5)	111.27(8)	O(3)−V(1)−O(4)	108.93(9)
O(3)−V(1)−O(5)	106.78(9)	O(4)−V(1)−O(5)	113.47(9)
O(1)−V(2)−O(2)	108.51(9)	O(1)−V(2)−O(2A)	107.37(9)
O(1)−V(2)−O(3A)	108.23(9)	O(1)−V(2)−O(5A)	106.64(8)
O(2)−V(2)−O(2A)	77.54(7)	O(2)−V(2)−O(3A)	87.60(7)
O(2)−V(2)−O(5A)	144.38(7)	O(2A)−V(2)−O(3A)	144.18(8)
O(2A)−V(2)−O(5A)	86.83(7)	O(3A)−V(2)−O(5A)	86.80(7)
N(1)−C(1)−C(1A)	109.8(3)		

(2)−1.824(2) Å and bond angles in the range of 105.64(8)−111.27(8)°. The $V(2)O_5$ square pyramid has bond distances in the range of 1.608(2)−1.970(2) Å. The major difference between the structures of **1a** and **1b** lies in the packing of the ethylenediammonium cations in the interlayer regions. In the structure of **1b**, each ethylenediammonium cation is centered at an inversion center at ($^1/_2$, 0, $^1/_2$) and stretches along the [101] direction. In the structure of **1a**, however, each ethylenediammonium cation is centered at an inversion center at (0, 0, 0) and is oriented in a direction nearly parallel to the *a* axis. This results in the expansion of the *a* axis and the shrinkage of the *c* axis in the structure of **1a** compared to those in the structure of **1b**. In addition, while the ethylenediammonium cations in the structure of **1a** are oriented almost parallel with respect to the oxide layers, those in the structure of **1b** are oriented with a small tilt angle with respect to the oxide layers. As a result, oxide **1b** has a larger interlayer distance of 7.246 Å, compared to 7.187 Å for **1a**.

The interlayer distance is increased to 7.773 Å when the interlayer ethylenediammonium cations are replaced by protonated piperazine cations as in the case of **2a**. However, the structure of the vanadium oxide layers of $V_4O_{10}^{2-}$ is retained as shown in Figure 5. Figure 6 shows the coordination environment around the two V atoms in the asymmetric unit

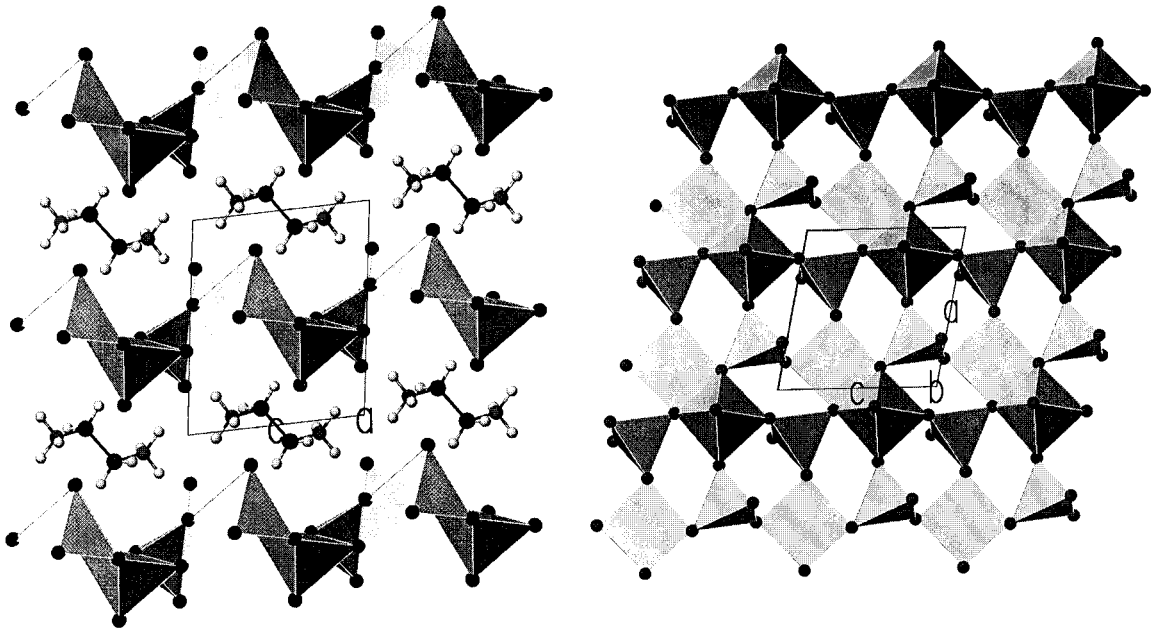

Figure 3. (left) View of the structure of **1b** down the *c* axis showing the layers of vanadium oxide and the ethylenediammonium dications in the interlamellar space. (right) View perpendicular to the oxide layer in the structure of **1b**.

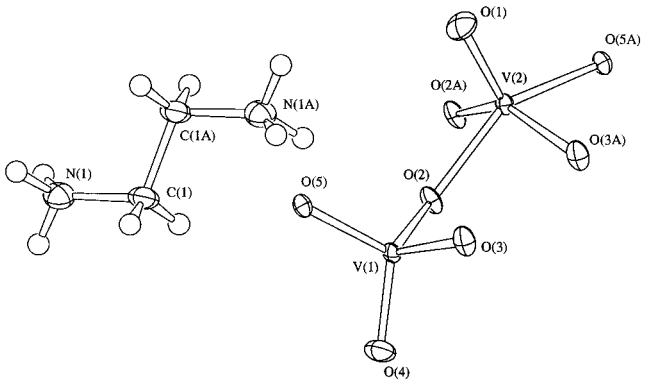

Figure 4. ORTEP drawing of the asymmetric unit in the structure of **1b** showing the coordination environment around the vanadium atoms. The atoms labeled with A and C are symmetry-related atoms.

and the numbering scheme used in Table 5 in which selected bond distances and angles are listed. The $V(2)O_4$ tetrahedron is quite regular, with bond distances in the range of 1.621(4)−1.837(3) Å and bond angles in the range of 105.7(2)−112.6(2)°. The $V(1)O_5$ group has a distorted-square-pyramidal configuration with bond distances in the range of 1.620(4)−1.968(3) Å. These configurations are typical for V^{5+} and V^{4+}. Valence sum calculations confirmed the oxidation state of the V atoms, which gave a value of 4.06 for V(1) and 4.75 for V(2). The piperazine cations are centered at an inversion center at ($^1/_2$, 0, 0) with a chair conformation. The N atoms are involved in hydrogen bonds with the terminal oxygens O(3) and O(5) from the adjacent oxide layers above and below with N- - -O distances in the range of 2.801(6)− 2.901(6) Å.

The structure of **2b** is shown in Figure 7, positional and thermal parameters are listed in Table 2, and selected bond distances and angles are given in Table 6. It has monoclinic symmetry, and the oxide layers run parallel to the (101) plane with an interlayer distance of 7.838 Å. The oxide layers are constructed from pairs of edge-sharing $V^{4+}O_5$ square pyramids connected together by $V^{5+}O_4$ tetrahedra via corner sharing. However, the pairs of the edge-sharing square pyramids are not uniformly oriented within the layer as they are in the structures of **1a**, **1b**, and **2a**. The rows of edge-sharing VO_5 square pyramids along the *b* axis have two different orientations and only repeat every other row along the [010] direction. Figure 8 shows the coordination environment around the V atoms. The $V(1)O_5$ distorted square pyramid has bond distances in the range of 1.622(3)−1.959(2) Å. The $V(2)O_4$ tetrahedron has bond distances in the range of 1.623(3)−1.852(3) Å and bond angles in the range of 102.6(1)−117.8(1)°. As seen from these bond angles, the distortion of the tetrahedron in this case is more profound as compared to those in the structures of **1a**, **1b**, and **2a**. Close examination of the oxide layer reveals that each $V(2)O_4$ tetrahedron has an additional weak V- - -O interaction with O(4) at a distance of 2.454 Å from another tetrahedron as shown by the arrows in Figure 7. This interaction constitutes about 18% of a V−O single bond and results in the expansion of the O(1)−V(2)−O(4) bond angle (117.8°) and the shrinkage of the O(2)−V(2)−O(4) bond angle (102.6°). However, there is no such weak V- - -O interaction in any of the structures of **1a**, **1b**, and **2a**, where more regular VO_4 tetrahedral bond angles are observed. The protonated piperazine cations which are centered at inversion centers at ($^1/_2$, $^1/_2$, 0) and (0, 0, $^1/_2$) have different orientations with respect to the oxide layers. The N atoms are involved in hydrogen bonds with the terminal oxygen atoms of O(3) and O(5) from the adjacent oxide layers above and below with N- - -O distances in the range of 2.867(5)−2.941(5) Å.

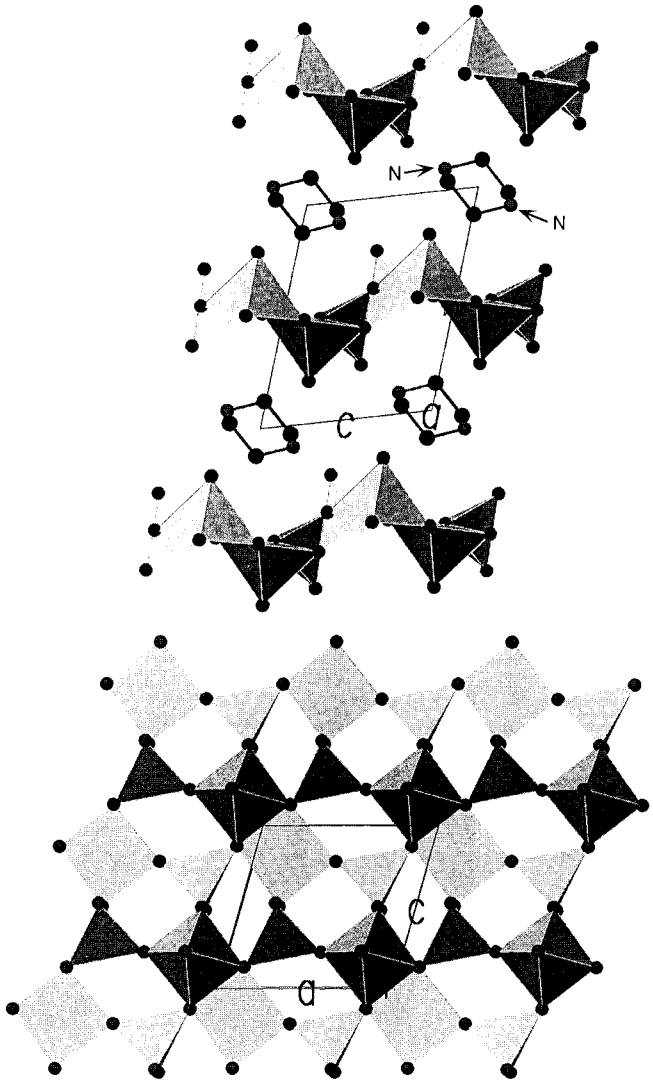

Figure 5. (top) View of the structure of **2a** down the *a* axis showing the layers of vanadium oxide and the protonated piperazine dications in the interlayer regions. The hydrogen atoms are omitted for clarity. (bottom) View perpendicular to the oxide layer in the structure of **2a**.

Thermogravimetric analysis (TGA) of these oxides (since it was not possible to separate phase **1a** from **1b** or phase **2a** from **2b**, the solid samples used in TGA were actually a mixture of **1a** and **1b**, or a mixture of **2a** and **2b**) showed, in both cases, no weight loss until ca. 300 °C, where a major weight loss begins to occur. This remarkable thermal stability of these oxides can be attributed to the strong hydrogen bond interactions of these organic molecules with the oxide layers. In the case of the mixture of **1a** and **1b**, the major weight loss in the temperature range of 310−380 °C was about 16%, and the sample continued to lose gradually 10% of its weight up to 610 °C. The first weight loss corresponds to the release of ethylenediamine with a calculated value of 14.1%. The TGA curve of the mixture of **2a** and **2b** shows the first major weight loss of 22% in the temperature range of 300−350 °C followed by a second loss of 4% at 400 °C and then no weight loss up to 800 °C, the highest temperature measured. The first weight loss corresponds to the release of piperazine with a calculated value of 19.0%. The nature of the second weight loss is not clear. However, it is likely that when the organic component is released, it leaves the protons behind attached to the oxygen atoms of the oxide layers, which are then released as water molecules at high temperatures.

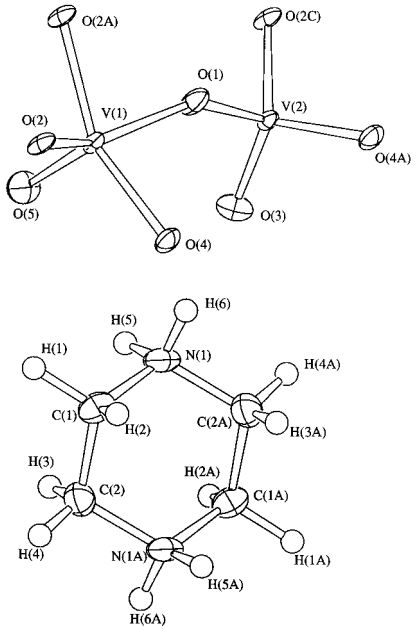

Figure 6. ORTEP drawing of the asymmetric unit in the structure of **2a** showing the coordination environment around the V atoms. The atoms labeled with A and C are symmetry-related atoms.

Table 5. Selected Bond Distances (Å) and Angles (deg) in the Structure of **2a**

V(1)−O(1)	1.913(3)	V(1)−O(2)	1.961(3)
V(1)−O(2A)	1.968(3)	V(1)−O(4)	1.926(3)
V(1)−O(5)	1.620(4)	V(2)−O(1)	1.697(3)
V(2)−O(2C)	1.837(3)	V(2)−O(3)	1.621(4)
V(2)−O(4A)	1.737(3)	N(1)−C(1)	1.482(7)
N(1)−C(2A)	1.482(7)	C(1)−C(2)	1.498(8)

O(1)−V(1)−O(2)	143.2(2)	O(1)−V(1)−O(2A)	87.1(1)
O(1)−V(1)−O(4)	87.6(1)	O(1)−V(1)−O(5)	107.3(2)
O(2)−V(1)−O(2A)	78.0(1)	O(2)−V(1)−O(4)	86.6(1)
O(2)−V(1)−O(5)	109.3(2)	O(2A)−V(1)−O(4)	146.1(1)
O(2A)−V(1)−O(5)	109.2(2)	O(4)−V(1)−O(5)	104.3(2)
O(1)−V(2)−O(2C)	106.0(1)	O(1)−V(2)−O(3)	108.4(2)
O(1)−V(2)−O(4A)	105.7(2)	O(2C)−V(2)−O(3)	112.6(2)
O(2C)−V(2)−O(4A)	111.6(2)	O(3)−V(2)−O(4A)	112.1(2)
C(1)−N(1)−C(2A)	112.1(4)	N(1)−C(1)−C(2)	109.8(4)
N(1A)−C(2)−C(1)	111.0(4)		

Discussion

Very recently Riou and co-workers[22] have isolated three amine intercalated vanadates from hydrothermal reactions of mixtures of $V_2O_5-SiO_2-HF-amine-H_2O$, two of which correspond to compounds **1b** and **2a** described here. The oxide layers in the four structures discussed here are compositionally and structurally related to that of V_2O_5, which has a pseudo-layered structure.[23] A schematic representation of the layer of V_2O_5 is shown in Figure 9. All the vanadium atoms in the structure of V_2O_5 are in the +5 oxidation state and have square-pyramidal configurations. These square pyramids share two edges with each other to form double chains along the crystallographic *c* direction, and these double chains of square pyramids are linked via corner sharing along the *a* direction perpendicular to the chains to form a two-dimensional layer. If one additional V−O bond is formed for each VO_4 tetrahedron (as indicated by the arrows in Figure 7) in the oxide layers of $[V_4O_{10}]^{2-}$, then all the vanadium atoms would have a square-pyramidal configuration, and all of these square pyramids share two edges to form double chains similar to those in the structure of V_2O_5. The structural correlations of $[V_4O_{10}]^{2-}$ with V_2O_5 have been discussed in more detail by Férey.[22] It should be pointed out that it is not necessary to use V_2O_5 as a starting material for the preparation of **1a** and **1b** which bear structural features similar to those of the parent compound V_2O_5. They can also be prepared using other vanadium sources such as $CsVO_3$, KVO_3, etc. The $V^{4+}O_5$ square-pyramidal and $V^{5+}O_4$ tetrahedral coordination configurations have often been observed

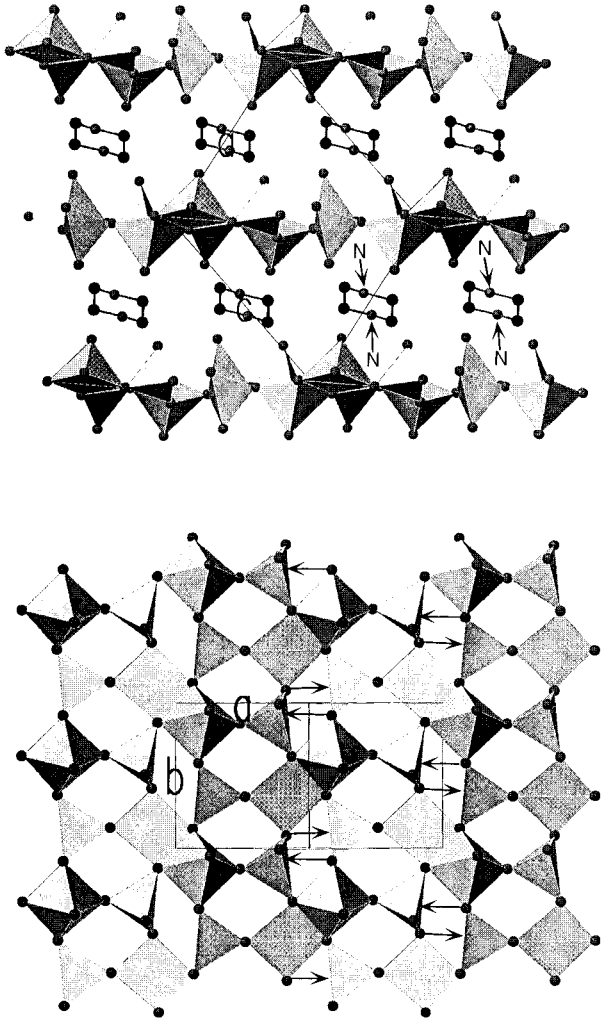

Figure 7. (top) View of the structure of **2b** down the *b* axis showing the layers of vanadium oxide and the protonated piperazine dications in the interlayer regions. (bottom) View perpendicular to the oxide layer in the structure of **2b**.

Table 6. Selected Bond Distances (Å) and Angles (deg) in the Structure of **2b**

V(1)−O(1)	1.956(2)	V(1)−O(1A)	1.959(2)
V(1)−O(2)	1.918(3)	V(1)−O(3)	1.622(3)
V(1)−O(4)	1.910(3)	V(2)−O(1)	1.852(3)
V(2)−O(2A)	1.707(3)	V(2)−O(4A)	1.768(2)
V(2)−O(5)	1.623(3)	N(1)−C(1)	1.467(6)
N(1)−C(2)	1.449(6)	C(1)−C(2A)	1.491(6)

O(1)−V(1)−O(1A)	77.5(1)	O(1)−V(1)−O(2)	144.1(1)
O(1)−V(1)−O(3)	109.1(1)	O(1)−V(1)−O(4)	82.4(1)
O(1A)−V(1)−O(2)	90.0(1)	O(1A)−V(1)−O(3)	109.0(1)
O(1A)−V(1)−O(4)	143.6(1)	O(2)−V(1)−O(3)	106.7(1)
O(2)−V(1)−O(4)	88.8(1)	O(3)−V(1)−O(4)	106.2(1)
O(1)−V(2)−O(2)	99.8(1)	O(1)−V(2)−O(4A)	117.8(1)
O(1)−V(2)−O(5)	114.7(1)	O(2A)−V(2)−O(4A)	102.6(1)
O(2A)−V(2)−O(5)	105.9(1)	O(4A)−V(2)−O(5)	113.4(1)
C(1)−N(1)−C(2)	114.1(4)	N(1)−C(1)−C(2A)	111.3(3)
N(1)−C(2)−C(1A)	113.2(4)		

(22) Riou, D.; Férey, G. *J. Solid State Chem.* **1995**, *120*, 137. Riou, D.; Férey, G. *Inorg. Chem.* **1995**, *34*, 6520.
(23) Enjalbert, R.; Galy, J. *Acta Crystallogr.* **1986**, *C42*, 1467.

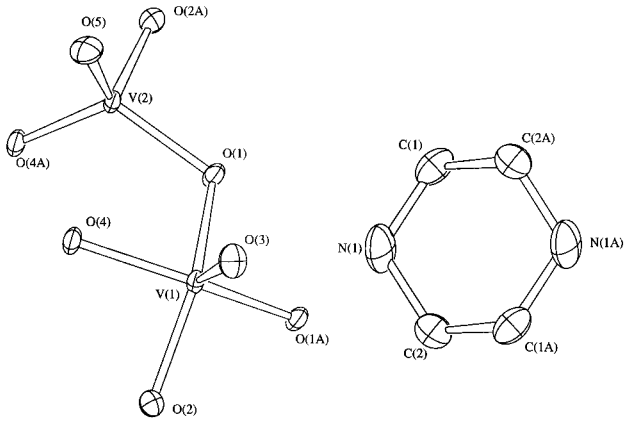

Figure 8. ORTEP drawing of the asymmetric unit in the structure of **2b** showing the coordination environment around the vanadium atoms. The hydrogen atoms are omitted for clarity. The atoms labeled with A and C are symmetry-related atoms.

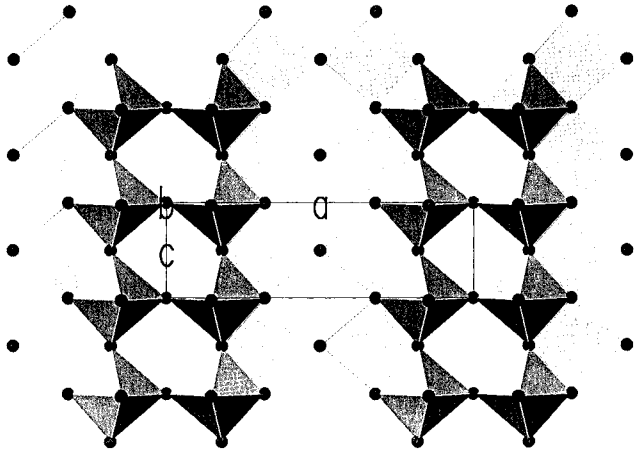

Figure 9. Polyhedral representation of the V_2O_5 layer in the crystal structure of V_2O_5.

in the structures of relatively alkali-metal-rich vanadium oxide bronzes such as $Cs_2V_5O_{13}$,[24] $A_2V_3O_8$ (A = K, Rb, Cs NH_4),[25] CsV_2O_5,[26] and $A_2V_4O_9$ (A = Rb, Cs).[27] The oxide layers in the structures of **1a, 1b, 2a,** and **2b** are similar to those in the structure of CsV_2O_5,[26] where the Cs^+ cations lie between the vanadium oxide layers. However, the terminal oxygen atoms of the VO_4 tetrahedra in the structure of CsV_2O_5 are oriented in a different way toward the opposite sides of the oxide layers.

In the intercalation reactions of $V_2O_5 \cdot nH_2O$ xerogel with alkylamines $C_nH_{2n+1}NH_2$ ($n = 1-18$),[4] it was found that the intercalates usually contain 0.3−0.4 mol of alkylamines/mol of V_2O_5. The alkyl chains of the amines in the interlayer regions were found to be oriented parallel, then tilted, and finally perpendicular to the host layers as the alkyl chain length increased. The intercalation mechanism probably involves a host-guest charge transfer. Partial reduction of V^{5+} to V^{4+} of the host layers has been also found in the intercalation reactions with ammonia,[6] pyridine,[6] benzidine,[7] and cobaltocenium cations $Co(C_5H_5)_2^+$.[28] It is interesting to note that an upper limit of 0.5 mol of alkylamine can be intercalated per mole of V_2O_5, as deduced from steric considerations. This turned out to be the case in the structures of oxides **1a, 1b, 2a,** and **2b** and the previously characterized sample of $(H_3N(CH_2)_3NH_3)[V_4O_{10}]$.[13,22] The oxide $(H_3N(CH_2)_3NH_3)[V_4O_{10}]$ has a layered structure similar to those of **1a** and **1b**. The interlayer regions are occupied by protonated diaminopropane cations. The oxide layers are constructed from VO_4 and VO_5 in a similar fashion. This compound undergoes an antiferromagnetic ordering at 25 K resulting from the antiferromagnetic d^1-d^1 coupling between the two edge-sharing $V^{4+}O_5$ square pyramids. In the structure of $(HN(C_2H_4)_3NH)[V_6O_{14}] \cdot H_2O$,[14] however, the oxide layers are constructed from infinite zigzag chains of edge-sharing $V^{4+}O_5$ square pyramids running parallel to the *b* axis, with their terminal vanadyl groups oriented in pairs toward opposite sides of the layers. These infinite chains are connected together by $V^{5+}O_4$ tetrahedra along the direction of the *c* axis, giving a layer composition of $[(V^{5+})_2(V^{4+})_4O_{14}]^{2-}$. In spite of the fact that this compound contains two thirds of the vanadium atoms in the 4+ oxidation state, an EPR signal was not observed. Preliminary magnetization measurements showed that it was essentially diamagnetic. Magnetic properties similar to those of $(H_3N(CH_2)_3NH_3)[V_4O_{10}]$ would be expected for **1a**, **1b**, **2a**, **2b**, considering their structural similarities. Unfortunately, we have not been able to prepare the oxides $(H_3N(CH_2)_2NH_3)[V_4O_{10}]$ and $(H_2N(C_2H_4)_2NH_2)[V_4O_{10}]$ in a single phase of α- or *β*- form, preventing us from performing a comparison study on the magnetic properties of these compounds.

Acknowledgment. The work at Texas A&M University was supported by the National Science Foundation under Grant No. DMR-9107715, for which grateful acknowledgment is made.

Supporting Information Available: Tables of crystallographic data, including additional experimental procedures, atomic coordinates for the hydrogen atoms, bond distances and angles involving the hydrogen atoms, and anisotropic thermal parameters for the non-hydrogen atoms (Tables S1−S5) (5 pages). Ordering information is given on any current masthead page.

IC951237C

(24) Waltersson, K.; Forslund, B. *Acta Crystallogr.* **1977**, *B33*, 784.
(25) Liu, G.; Greedan, J. E. *J. Solid State Chem.* **1995**, *114*, 499. Andrukaitis, E.; Jacobs, P. W. M.; Lorimer, J. W. *Can. J. Chem.* **1990**, *31*, 101.
(26) Waltersson, K.; Forslund, B. *Acta Crystallogr.* **1977**, *B33*, 789.
(27) Liu, G.; Greedan, J. E. *J. Solid State Chem.* **1995**, *115*, 174.
(28) Aldebert, P.; Paul-Boncour, V. *Mater. Res. Bull.* **1983**, *18*, 1263.